Study of channel instability in the braided Brahmaputra river using satellite imagery

Tapas Karmaker[1,*], Hemanta Medhi[2] and Subashisa Dutta[3]

[1]Department of Civil Engineering, Thapar University, Patiala 147 004, India
[2]Department of Civil Engineering, Indian Institute of Technology Kanpur, Kanpur 208 016, India
[3]Department of Civil Engineering, Indian Institute of Technology Guwahati, Guwahati 781 039, India

In the present study, instability of the river reach of Brahmaputra was analysed for braided belt width changes, braiding index and bar area. The river reach of the Brahmaputra from its confluence of Lohit, Dibang and Dihang to its confluence with the Tista river was studied from 1973 to 2009. The study was carried out using remotely sensed data from Landsat satellites at different dates. Discharge data synchronized with satellite data was collected by maintaining near-similar water level or discharge. Wavelet of the braided belt change was analysed to get the wavelet power and spatial extent of the changes. Finally, stream power was analysed from the average discharge data during the monsoon period to determine its effect on the instability of parameters considered. Results indicate that stream power does not directly relate to local changes in the braided belt or braiding index. However, with decrease in stream power, an increasing trend of bar area was found. Maximum wavelet power within a period showed a threshold behaviour at stream power of 5 W/km, beyond which the wavelet power raised sharply to a high value with increase in stream power. River response to the stream power was found at a global level rather than local level. Finally, a gradual decrease in stream power over time indicates the stable river reach. However, changes due to local bank erosion cannot be predicted using this analysis.

Keywords: Braiding index, braided belt, plan form, stream power.

BRAHMAPUTRA river is one of the world's largest, braided and dynamic river systems. The dynamics of the river are attributed to high rates of riverbank erosion, increase in braided belt, change in channel courses and braiding pattern[1]. Also, due to high rates of bank erosion and frequent changes in the channel flow, it becomes difficult to take efficient river training measures[2]. It is therefore necessary to understand the dynamics of the river and identify the stable and unstable reaches through temporal analysis. Continuous monitoring of river's morphological changes can be considered as a cost-effective measure for efficient management system of the bank erosion problem[3]. For an efficient morphological study of Brahmaputra river, spanning over hundreds of kilometre length, it is necessary to carry out multi-date satellite remote sensing data analysis.

Brahmaputra flows a total distance of approximately 2900 km from its origin at Manasarovar (Tibet) to Bay of Bengal. The river mainly flows from east to west (in India) up to the Indo-Bangladesh border and then from north to south (in Bangladesh). The braided belt varies considerably from ~1.3 km at Pandu (near Guwahati) to 18.5 km near the Indo-Bangladesh border as studied with the help of Landsat-7 satellite imagery in 2009. Notably, the narrowest reach (Pandu) of the river is bedrock-controlled and hence no bank erosion was evident. The river flows through the Himalayan valley which is composed of Paleozoic sediments[4]. The eastern side and the southern side (Sillong Plateau) of the river are composed of high-grade metamorphites, gneiss, schists and granites overlain by metasediments[4,5]. The south-eastern side of the river basin is composed of sandstones, shales and mottled clays which are easily erodible. The longitudinal bed slope varies from 1 in 3000 near Passighat to 1 in 12700 near Dhubri[6]. The high annual rainfall (100–600 cm) in this river basin is linked with high magnitude floods (bank full stage and higher) during monsoon every year. The discharge of the river varies widely from 1757 $m^3 s^{-1}$ (20 February 1968) to a maximum of 72,984 $m^3 s^{-1}$ (23 August 1962) as recorded at Pandu (Guwahati) gauging station.

Bankline migration and fluvial erosion of Brahmaputra have been studied earlier[7–11] with Survey of India toposheets and/or satellite imagery. Recent studies on river morphology have extensively used satellite remote sensing imagery[3,12–17]. Takagi *et al.*[18] studied the river reach of Brahmaputra in Bangladesh and concluded that the river is in dynamic equilibrium stage with its stabilization waves propagating to the downstream. Baki and Gan[14] reported that the larger sandbars in Brahmaputra are more stable than the smaller ones. Akhtar *et al.*[3] examined the stream power relation with braiding pattern and concluded that with low stream power, braiding intensity increases, which in turn intensify bank erosion. Lahiri and Sinha[16] carried out a geomorphologic study of Majuli

*For correspondence. (e-mail: tapas1976@gmail.com)

island of Brahmaputra and concluded that the channel planform processes are related to the tectonic activity of the locality. In another study, Lahiri and Sinha[17] used fast fourier transform (FFT) of the bank lines to identify the regional and local control of the bank erosion. Recently, Chembolu and Dutta[19] studied the Brahmaputra river morphology disorder in relation to entropy and found that four-year return period flood causes disorder in the river planform which in turn increases entropy.

Despite these studies, there is limited understanding of the relations of stream energy and channel instability of a large river system. In the present study, an attempt has been made to relate the river dynamics of Brahmaputra with braiding index, braided belt and unit bars by using multi-date satellite imagery and the Survey of India toposheets.

Study area

The study reach of Brahmaputra river, approximately 750 km long from the confluence of Lohit, Dibang and Dihang in Assam near Kobo (27°47′N, 92°25′E) until its confluence with the Tista river, is considered in the present study (Figure 1). The median bed-material size is 0.20 mm (ref. 20). Brahmaputra carries a high average sediment load of 2.0×10^6 tonnes/d between June and September every year[21]. The majority of the load is suspended sediment and only 5–15% of the load is bed load[5]. The average suspended load was estimated to be 402×10^6 tonnes/y (ref. 21); while the average suspended sediment concentration was reported to be about 460 mg/l (ref. 20). Figure 2 shows the longitudinal bed profiles of the river in 1971, 1977 and 1981 (ref. 22). The bank's soil of the river is highly erodible[23] and various reaches of the Brahmaputra river experience severe bank erosion during and after the monsoon every year due to seepage and fluvial erosion[24,25].

Data and methods

For the fluvial and morphological study, one set of Survey of India (SOI) toposheets (1944) and a total of 28 Landsat-Multi Spectral Scanner (MSS) (spatial resolution 80 m), Landsat-Thematic Mapper (TM) (spatial resolution 30 m) and Landsat-Enhanced Thematic Mapper+ (ETM+) (spatial resolution 30 m) satellite imagery covering the whole Brahmaputra river in Assam were selected. Each of the satellite images comprised 7 scenes. All satellite images were collected during the non-monsoon period (November–March) of 1973, 1990, 2000 and 2009 respectively. During this period, it is more likely to obtain almost cloud-free images with consistent vegetation cover and water levels year to year. The toposheets were prepared at a scale of 1 : 250,000. These toposheets were divided in 1.5° longitudinal and 1° latitudinal grid. A total of 14 digitized toposheets were initially geo-referenced by using 15 ground control points (GCPs) from the scanned hard copy map and second order polynomial function. The nearest neighbourhood re-sampling technique was used. The average root mean square (RMS) error during these geo-referencing was found to be less than one pixel (pixel size 0.5″ × 0.5″). The geo-referenced toposheets and the satellite imagery were mosaicked separately to obtain the study river reach for different years. To bring all the images (toposheets and satellite imagery) under an identical geometric projection system, these were geo-referenced with respect to Landsat-ETM+ image of the year 2000 by using universal transverse mercator (UTM) projection and world geodetic system 84 (WGS) ellipsoid. Geo-referencing was done by using: (1) at least 24 GCPs for each scene of Landsat images and toposheets; and (2) second-order polynomial with nearest neighbourhood re-sampling technique with RMS less than 0.5 pixel, while the pixel size adopted was 30 m × 30 m. The analysis and geo-referencing were carried out using GEOMATICA®, a digital image processing software.

The discharge and water level data of the Brahmaputra river was collected from gauging stations at Pandu (near Guwahati) in the years 1973, 1990, 2000, 2009 (Figure 3). The water level varied between 44.6 and 46.0 m in different years.

Riverbank shifting was detected based on visible and near infra-red (NIR) bands of Landsat images. For convenience of analysis, the river was divided at 10 km intervals, 73 reaches. Each reach was assigned with a chronological identification number. The permanent reference line of lat. 27°47′N and long. 92°25′E at the upstream of the study reach was taken. Identification of the banklines in Brahmaputra was not difficult in most cases, but the inclusion of abandoned channels within the braided belt was ambiguous. To eliminate this difficulty, the criterion adopted by EGIS[26] was followed. The sand bodies except sediments splayed over flood plains were considered within the braided belt. The overflanking channel <100 km was also considered within the braided belt[14]. The banklines and channel lines were detected using normalized difference water index (NDWI) images. The NDWI images were prepared from the multi-spectral satellite data using the formula

$$\mathrm{NDWI} = \frac{\mathrm{NIR} - \mathrm{SWIR}}{\mathrm{NIR} + \mathrm{SWIR}}, \quad (1)$$

where SWIR is the reflectance of short wave infra-red band. NDWI is a measure of moisture content. NDWI increases either with vegetation water content or from dry soil to free water. NDWI is a useful tool to identify the bank lines[27]. Shallow water channels were considered as part of the river. Old and new sand deposits at the river

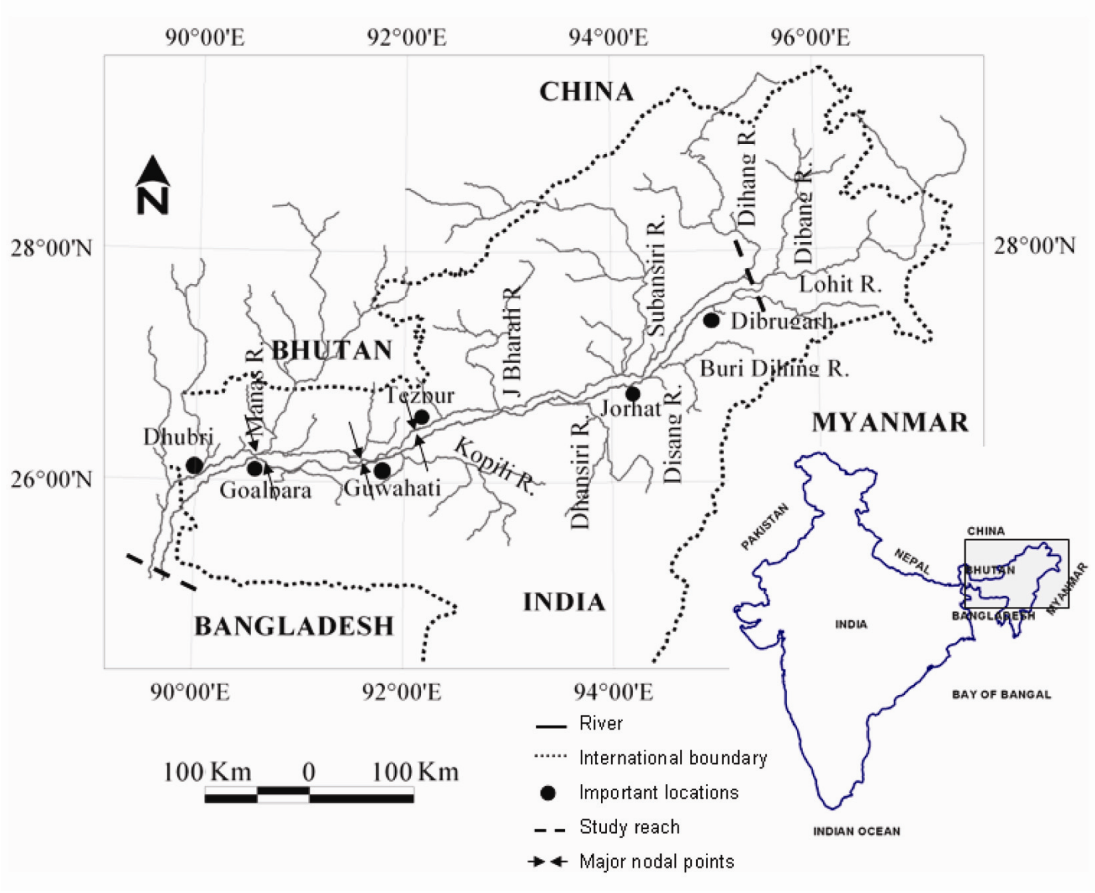

Figure 1. Location of the study area and major nodal points.

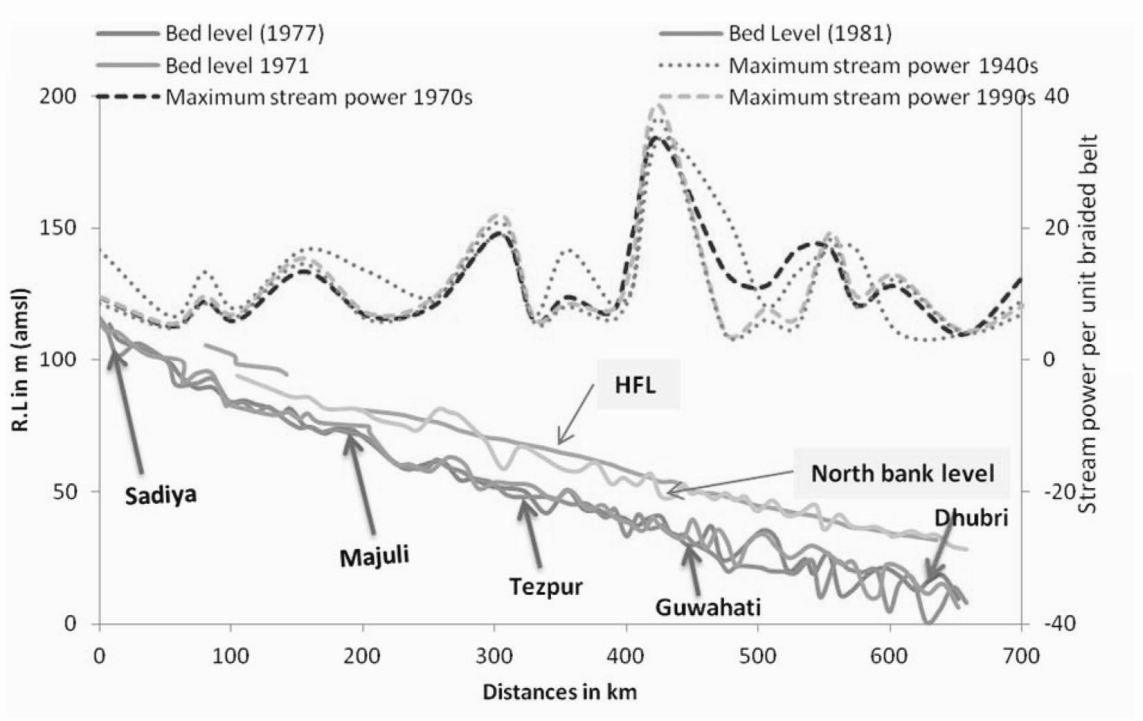

Figure 2. Longitudinal profile and unit stream power of Brahmaputra river at various time period (stream powers per unit width are measured in W/km).

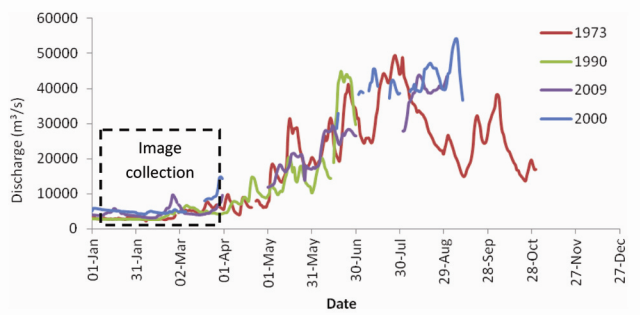

Figure 3. Image collection period and discharge at different years.

banks sometimes pose confusion if they were included within the river. The sand patches with moisture content indicate the presence of river water, whereas sand deposits with low moisture content or dry soil indicate absence of river water. Subsequently, sand deposits were not considered within the river if NDWI was very low. A similar method was followed to identify sand bars. The bankline migration rates were estimated based on the differences between two available consecutive NDWI images.

The study reach was sub-divided into 73 segments each with 10 km long except first and last segments. Thorne *et al.*[12] reported that the scales of planform evolution of the Brahmaputra river were spaced at intervals of approximately 30 km. To capture this scale, a length segment of 10 km was adopted. The first and last segment lengths vary in order to incorporate the shifting of the river confluence during this period. Each segment was assigned a chronological identification number to compare the segment temporally. For convenience, the distances along the river were measured from the confluence (1940s) at the upstream and expressed in km. The area within a segment divided by the length of that segment gives the average braided belt width (B_b) in the corresponding section and subsequently used for analysis.

To identify the dynamics of the braided belt for different spatial and temporal scale, continuous wavelet transformation (CWT) was performed for braided belt width. The spatial or temporal series can be transformed into two-dimensional space or time frequency relations. CWT can be defined by $W(s, \sigma)$ with its 'mother' wavelet function or basis function $\psi_{x,\sigma}$ as

$$W(s,\sigma) = \int_{-\infty}^{\infty} y(x)\psi_{x,\sigma}(x)\mathrm{d}x, \tag{2}$$

$$\text{where} \quad \psi_{x,\sigma} = \frac{1}{\sqrt{s}}\psi\left(\frac{x-\sigma}{s}\right), \tag{3}$$

where s is the dilation or scale of wavelet function and σ is the degree of distance translation along the series. For details, reader can refer to the work by Torrence and Compo[28]. CWT was successfully applied by Mount *et al.*[29] for bank erosion scale analysis. Mount *et al.*[29] concluded that out of three different basis functions, the Morlet function with order 3 was the best, that clearly resolves different spatial scales. Therefore, in this study, we used Morlet as the basis function

$$\psi(x) = \pi^{-1/4} e^{ikx} e^{-x^2/2}, \tag{4}$$

where k is the wavelet order (= 3 in the present study).

To characterize the braiding pattern, the braiding index (BI) proposed by Brice[30] is used in this study

$$\mathrm{BI} = 2\,\Sigma L_i / L_r, \tag{5}$$

where ΣL_i is the length of the all the unit bars within the strips of 10 km and L_r is the length measured along the centre line of the channel.

The river morphology is often governed by the unit stream power of the river. Unit stream power of a river channel can be given as

$$\Omega = \gamma QS / w, \tag{6}$$

where γ is the specific weight of water, Q the discharge, S the longitudinal slope of the channel and w is the width of the channel. For maximum stream power, the maximum peak discharge in a decade was considered with average width in that decade, whereas the average decadal discharge was considered to determine the decadal average stream power.

Results and discussion

Spatio-temporal variation in braided belt

The braided belts measured for each reference segment totalling 73 in numbers are plotted in Figure 4. It can be observed that during the period between 1943 and 1973 the braided belt increased at all cross-sections. The rate of increase in the braided belt was higher at upstream of Tezpur (from reach 1 to 30) than downstream. The maximum increase of the width in this period was 5.61 km between reach numbers 11 and 15 (near Jorhat town, Assam). The mean rate of decadal increase was 750 m from 1943 to 1973, 500 m from 1973 to 1990 and 760 m from 1990 to 2000. The abnormal decadal increase of 6.5 km in the belt was caused by the formation of anabranching at reach 47 between 1973 and 1990 but remained stable during 1990–2000. Minor changes in braided belt were noticed in reach numbers 55 to 73 during years 1943 to 1973. Later, the braided belt increased gradually from 9.02 to 11.35 km from 1973 to 2000. Stable reaches were also observed at reach numbers 45 and 46 during 2000 and 2009.

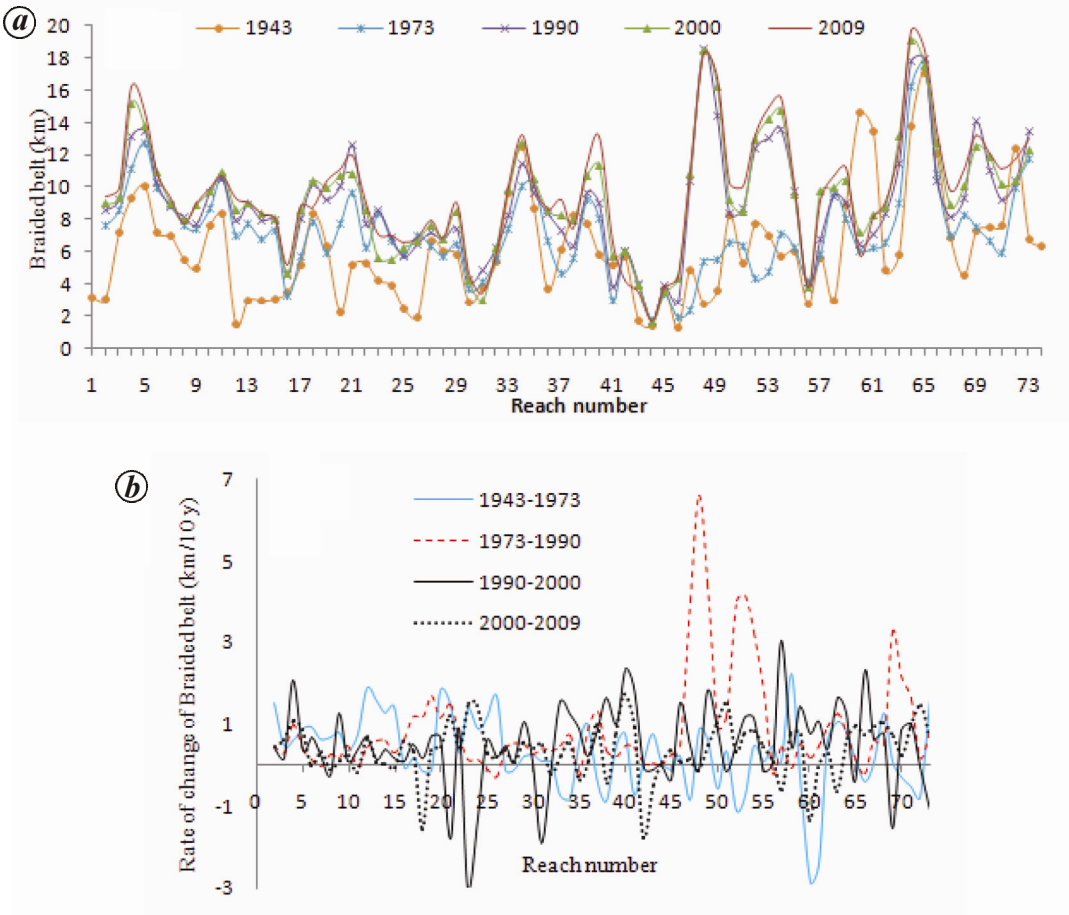

Figure 4. ***a***, Reachwise braided belt at different years. ***b***, Decadal changes in braided belt.

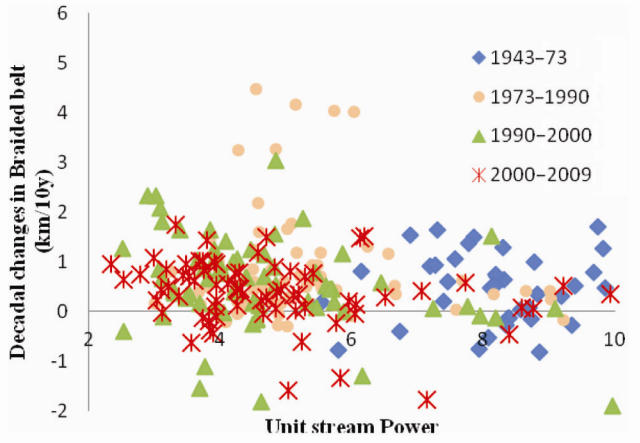

Figure 5. Relationship between unit stream power and braided belt.

The stream power of the river reach for 1940s, 1970s, 1990s and 2000s was calculated based on the maximum annual discharge and annual average discharge in each period. The maximum unit stream power indicates temporal variation at different reaches (Figure 2). The peak discharge higher than three-year return period along with braided belt at that period is shown in Table 1. It was found that in 1940s, the average unit stream power was high in most of the reaches (Figure 5). Gradually, with increase in the braided belt, the unit stream powers decreased in most of the reaches and from 1990s onward, the average unit stream power is almost stable within the study reaches (Table 2).

Wavelet analysis of braided belt width

During 1940–1970, the wavelet analysis resolved wave periods of 8 km (Figure 6). Significant zones were not discrete and spread almost throughout the reaches. However, locally significant zones were found for longer stretches at 200–500 km and 500–700 km. From 1970s–1990s, wave periods of 4 km were found (Figure 6 *a*). Only one significant erosion zone was identified and spread from 400 to 550 km reach. From 1990s to 2000s, wavelet analysis showed wave period of 4 km or less (Figure 6 *a*). Significant zones were extended over substantial downward distance. These were coupled with locally discrete shorter wave period zones. Significant zones were extended from 150 to 400 km and from 400 to 700 km. In the next period, from 2000 to 2009, wave period of 4 km or less was found. Spatially discrete

Table 1. Morphological changes in relation with flood events (numerals within bracket indicate standard deviation). Distances are measured from upstream to downstream

Period	Peak annual discharge $\times 10^4$ (m^3/s)	Year	Return period (year)	Data	Average braided belt (km)				Average Brice index				Average number of channel bar			
					0–305 km	305–450 km	450–550 km	550–735 km	0–305 km	305–450 km	450–550 km	550–735 km	0–305 km	305–450 km	450–550 km	550–735 km
Up to 1940s	–	–	–	SOI	5.11 (2.27)	6.82 (2.98)	4.64 (2.29)	8.96 (4.12)	3.55 (2.16)	4.86 (2.55)	3.09 (1.90)	5.37 (3.29)	6.22 (4.26)	7.55 (3.67)	4.31 (2.36)	8.29 (5.22)
1940s–1970s	5.25	1955	3.0	MSS	7.36 (2.08)	6.82 (2.43)	4.59 (1.82)	9.02 (3.47)	3.84 (2.14)	4.29 (2.01)	2.70 (1.30)	6.41 (3.88)	5.65 (3.26)	5.45 (2.50)	4.46 (2.63)	8.47 (4.47)
	5.23	1956	3.0													
	5.80	1957	9.0													
	6.20	1958	18.0													
	5.30	1959	3.1													
	5.80	1960	9.0													
	5.20	1961	3.0													
	7.25	1962	100													
	4.73	1963	3.0													
	5.90	1964	9.0													
	5.80	1966	9.0													
	4.90	1970	3.0													
	5.10	1973	3.1													
	5.28	1974	3.2													
	4.82	1975	3.0													
1970s–1990s	5.28	1977	3.2	TM	8.35 (2.26)	7.65 (2.39)	9.35 (5.14)	10.62 (3.43)	4.97 (2.65)	3.68 (1.84)	4.32 (2.65)	6.68 (4.26)	8.52 (4.59)	6.27 (3.10)	6.62 (3.93)	13.24 (9.69)
	5.10	1978	3.1													
	5.40	1980	5													
	5.10	1984	3.1													
	5.20	1987	3.15													
	6.05	1988	10.0													
1990s–2000s	4.82	1990	3.0	ETM	8.49 (2.59)	8.68 (2.67)	9.86 (5.36)	11.35 (3.10)	5.02 (3.13)	5.15 (2.95)	5.82 (3.61)	8.09 (3.90)	8.77 (5.23)	9.00 (4.17)	9.31 (6.71)	15.65 (9.43)
	5.75	1991	7.0													

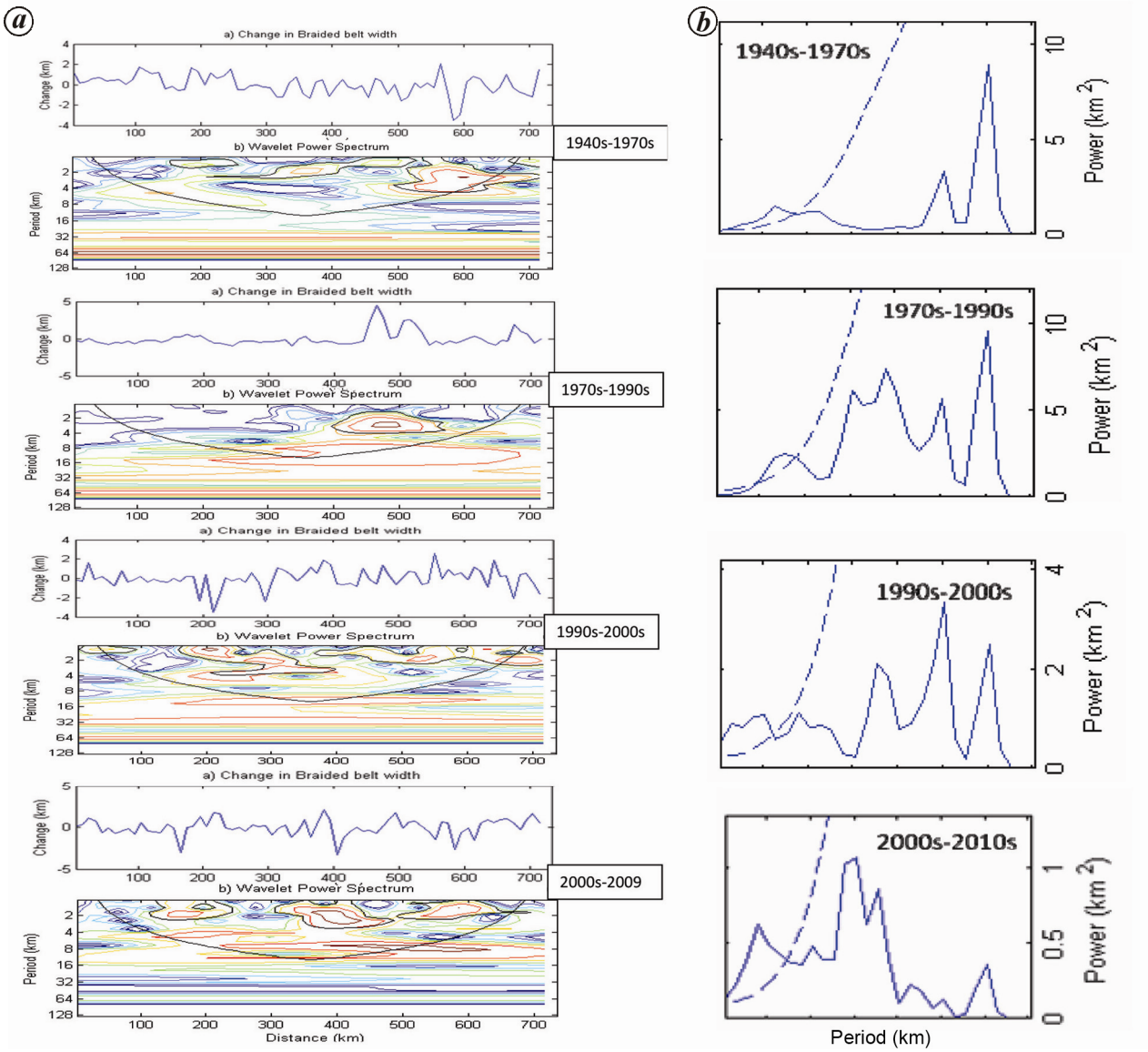

Figure 6. ***a***, Wavelet analysis of the decadal braided belt change. ***b***, Wavelet power spectrum at different periods.

Table 2. Mean and standard deviation for stream power in the study reach

Period	Mean	Standard deviation
1943–1973	10.54	3.79
1973–1990	5.70	2.29
1990–2000	4.99	2.31
2000–2009	4.92	2.08

significant wave periods were found. Significant zones were extended from 100 to 200 km, 300 to 450 km and 450 to 650 km. Higher wave period indicates global controls while lower period indicates local or regional controls[17]. The analysis clearly shows that during the period 1940–1970, the braided belt was controlled more globally rather than locally whereas during later periods the river-braided belt was controlled more locally, most probably with local erosion deposition mechanism.

Temporal variation of braiding index

The braiding index shows increasing and decreasing pattern along the river reaches (Figure 7). The maximum and minimum index was estimated to be 12.36 and zero in 1940s, 16.19 and 0.07 in 1970s, 16.30 and zero in 1990s and 17.84 and 0.33 in 2000s. An index of zero indicates non-braided river reach, which was found in the Brahmaputra river near Guwahati. During this period, the maximum index was found at 650 km. However, SOI data show that at 130 and 160 km, the index was also zero. The average index was 4.0 in 1940s, increased to 4.3 in 1970s, 5.06 in 1990s and 5.9 in 2000s. The

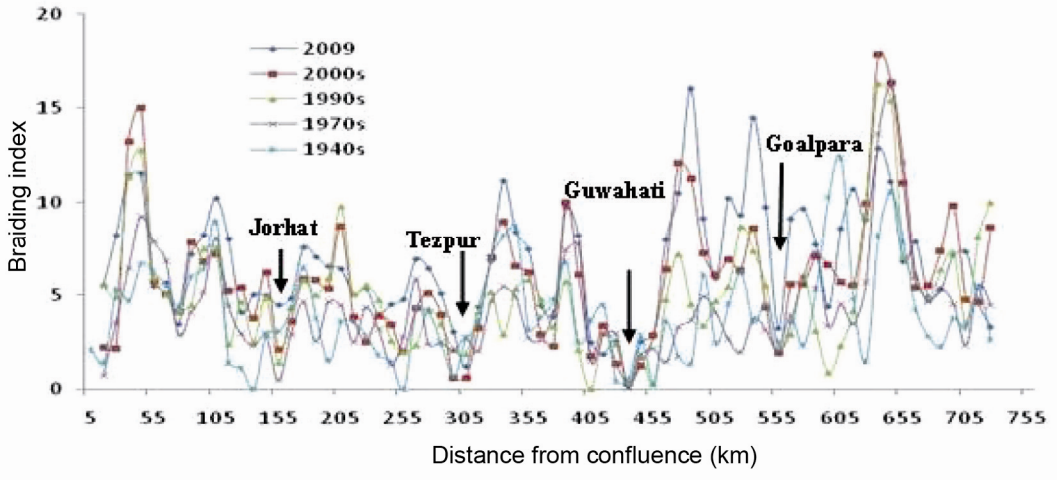

Figure 7. Braiding index in various years (distances are from upstream confluence).

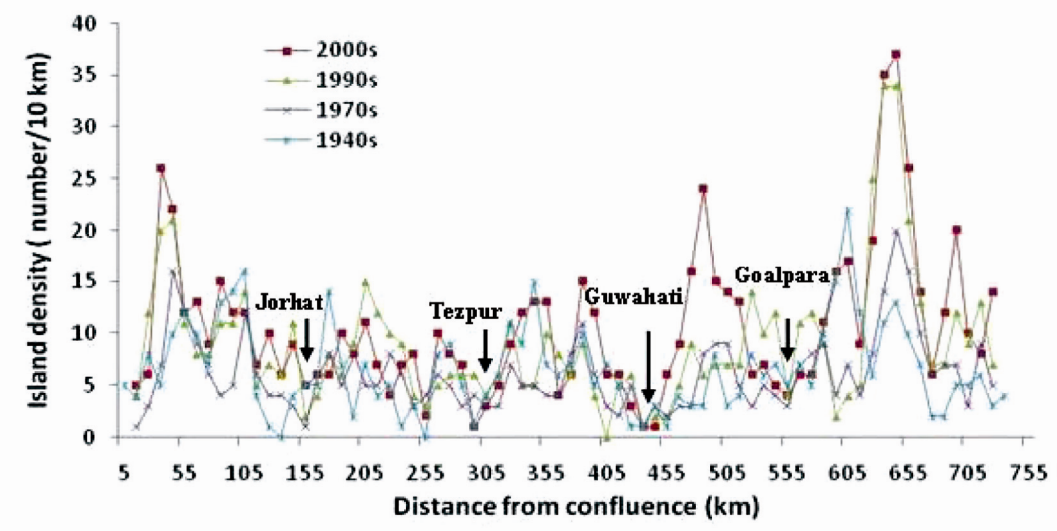

Figure 8. Temporal changes in mid channel island (or bar) density.

standard deviation increased similarly from 2.57 in 1940s to 3.55 in 2000s.

Temporal variation of unit bar area

Due to variation in annual discharge, significant morphological changes within a year in Brahmaputra could be noticed[2]. The changes were expressed in terms of bar density and bar area. Figure 8 shows the variation in bar (island) density in the study reach for the four time periods. During 1940s and 1970s the average bar density ranged between 6.5 and 6.0 bars/10 km. After that, the average density increased continuously and was 8.9 bars/10 km in 1990s and 10.5 bars/10 km in 2009. A similar increasing trend was found in standard deviations (4.3, 3.6, 6.3 and 7.0 bars/10 km in 1940s, 1970s, 1990s and 2000s respectively). The maximum bar density was about 35 bars/10 km in 2000s at 650 km. Only at the major nodes the bar density was restricted to 0–1 bar/10 km during the study period.

The frequency distributions of the bar (island) area were computed and shown as cumulative probability of the size of bars for each period (Figure 9). An anomaly in the trend was noticed from 1940s and 1970s. It may be noted that the cumulative distribution of bar sizes of 1940s and 1970s data did not match with 100% similarity. This is due to larger number of large bars (>13 km²) that were found during these periods. The distribution curve of 1990s indicates that there was a trend of smaller bar size. Interestingly, the cumulative probability of 2000s bar size showed good match with that of 1990s.

Stream energy analysis and channel stability

Figure 5 shows the effect of unit stream power (based on annual average discharge) on the decadal changes of

braided belt. Generally, it is expected that river bed/bank erosion will be proportional to unit stream power[31]. However, the present study does not support a similar hypothesis. During 1943–1973, unit stream power was high (6–10 W/km) with decadal changes from ~ –1 to +2 km. However, during 1973–1990, with low stream power (4–6 W/km) high decadal changes in braided belt (~ +5 km) was found. In the next period from 1990 to 2000, unit stream power varied from 2 to 10 W/km with low decadal changes (–2 to +3 km) in braided belt width. From 2000 to 2009, a similar anomaly was found; the steam power varied from 2 to 10 W/km but the decadal changes were recorded as –2 to +2 km.

Figure 10 shows the typical plot of reach-wise unit stream power (based on annual average discharge) and rate of change in decadal braided belt during 2000–2009. At few reaches (e.g., 17, 23, 29 and 42), decadal changes in braided belt were high with high unit stream power. But in most of the cases, the figure shows that though the unit stream power was high, decadal changes were out of phase.

The analysis of decadal changes in braiding index indicated that when the unit stream power was in the range of 2–6 W/km, decadal changes in the braiding index were high (Figure 11). With further increase in unit stream power a fall in the decadal changes of BI was noticed.

Figure 12 shows four different cases with average unit stream power in the study reach and the decadal changes of bar area. The unit stream power was found not to be related to the bar area changes. Even with high unit stream power, the bar area changes were minimum (~–10 km^2; negative value indicates wash out of the bars), but rather high value (~350 km^2) with unit stream power of 5 W/km.

In the previous section, the wavelet analysis of changes in braided belt was reported. The maximum power spectra and average unit stream power during the four-study period were shown in Figure 13. The figure indicates that when the average unit stream power was high, the maximum wavelet power was also high. When the average unit stream power was nearly 5 W/km, there was a sudden jump in wavelet power from ~1 to 10 and remained high with higher unit stream power. Hence, wavelet power can be considered to have a relation with the average unit stream power. Average stream power of 5 W/km can be taken as a threshold for the maximum wavelet

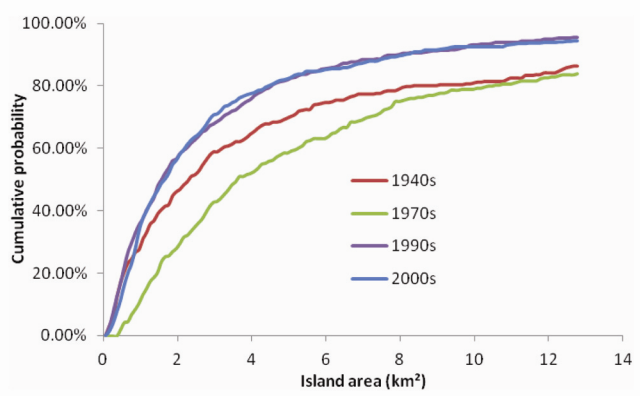

Figure 9. Cumulative frequency distribution of the channel bar (island) area during the study period.

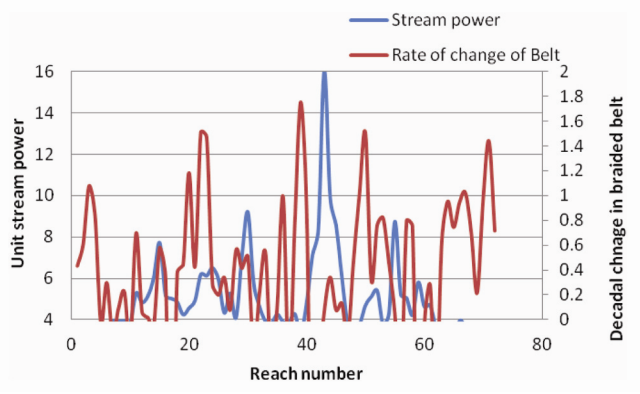

Figure 10. Typical plot of stream power and decadal changes in braided belt.

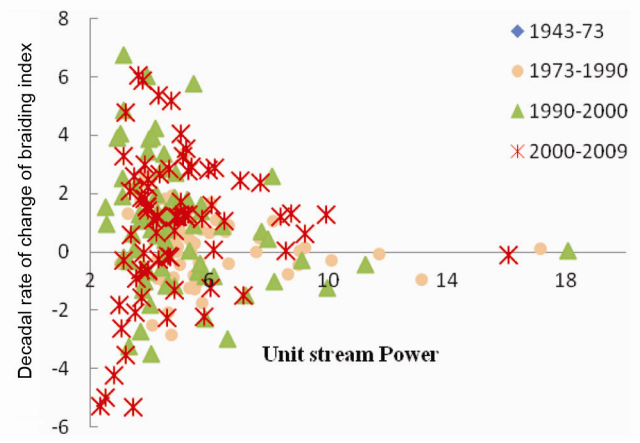

Figure 11. Relationship between unit stream power and decadal changes in braiding index.

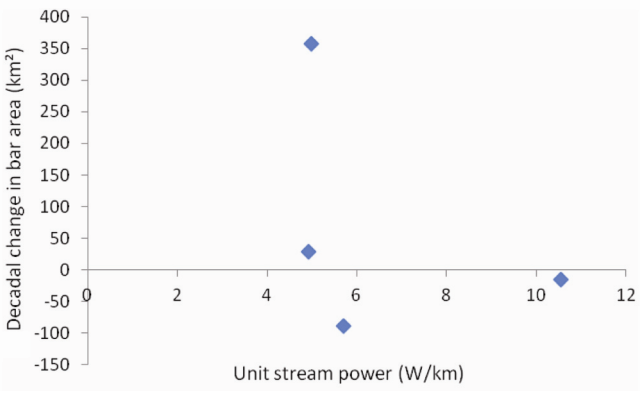

Figure 12. Relationship between unit stream power and bar area.

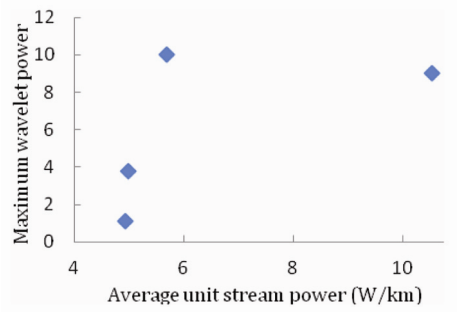

Figure 13. Relationship between unit stream power and wavelet power.

power beyond which higher wavelet power is expected with high unit stream power in a river reach.

Conclusion

In the present study, a detailed instability analysis of Brahmaputra river was carried out. Four study periods: 1943–1973, 1973–1990, 1990–2000 and 2000–2009 were considered. The river reach of Brahmaputra from its confluence of Lohit, Dibang and Dihang to its confluence with the Tista river was studied during these periods. Three parameters important in a braided river were considered: spatio-temporal variation in the braided belt, temporal variation of unit bar area and the temporal variation of the braiding index. Results indicate an increase in braided belt width of the river from 1943 to 1973 and in the later period, the changes gradually decreased. The unit stream power was also high during 1943–1973, which gradually decreased later. A gradual increasing trend of bar density was noticed from 1943 to 2009.

Interestingly, it was found that stream power neither directly controls braided belt movement, nor the braiding index. Even the stream power is not directly related to the unit bar area. With a low stream power, increase in bar area was found from the study. However, the wavelet power spectrum of braided belt change showed a threshold behaviour at unit stream power of 5 W/km, above which the wavelet power suddenly increased to a high value. In the above mentioned analysis, there were two local parameters (braided belt and braiding index) and two global parameters (bar area in the river and maximum wavelet power). The responses of local parameters to the unit stream power were poor and no direct relationship was found in this study. However, responses of the global parameters to the unit stream power indicated relationships. It can be concluded that, local changes in river morphology are not directly related to local stream power; however, river responses to the average stream power, globally. Further, as was found from the analysis, the unit stream power decreases over time during the study period, hence global stability can be expected from the river in near future. It can also be noted here that bank erosion or braided belt movement is governed by local hydraulic and erosion-deposition mechanism and hence, these cannot be predicted from the stream power relationships.

1. Dutta, S., Medhi, H., Karmaker, T., Singh, Y., Prabhu, I. and Dutta, U., Probabilistic flood hazard mapping for embankment breaching. *ISH J. Hydral. Eng.*, 2010, **16**(SP 1), 15–25.
2. Karmaker, T. and Dutta, S., Prediction of short-term morphological change in large braided river using 2D numerical model. *J. Hydraul. Eng.*, 2016, **142**(10), 04016039(1–13); doi:10.1061/(ASCE)HY.1943-7900.0001167.
3. Akhtar, M. P., Sharma, N. and Ojha, C. S. P., Braiding process and bank erosion in the Brahmaputra River. *Intl. J. Sediment Res.*, 2011, **26**, 431–444.
4. Sarma, J. N., Fluvial process and morphology of the Brahmaputra River in Assam, India. *Geomorphology*, 2005, **70**, 226–256.
5. Talukdar, N. C., Bhattacharyya, D. and Hazarika, S., Soil and agriculture. In *The Brahmaputra Basin Water Resources* (eds Singh, V. P., Sharma, N. and Ojha, C. S. P.), Kluwer Academic Publishers, The Netherlands, 2004, pp. 35–71.
6. Sarma, J. N., An overview of Brahmaputra river system. In *The Brahmaputra Basin Water Resources* (eds Singh, V. P., Sharma, N. and Ojha, C. S. P.), Kluwer Academic Publishers, The Netherlands, 2004, pp. 72–87.
7. Sarma, J. N., A Study on pattern of erosion and bankline migration of the River Brahmaputra in Assam using GIS. Report Disaster Management in North-Eastern region. Dept. of Revenue, Govt of Assam, 2002, pp. 50–53.
8. Sarma, J. N., Pattern of erosion and bankline migration of the river Brahmaputra in Assam using remote sensing data. Unpublished project report, Dibrugarh Univ., 2004, p. 200.
9. Gilfellon, G. B., Sarma, J. N. and Gohain, K., Channel and bed morphology of a part of the Brahmaputra river in Assam, India. *J. Geol. Soc. India*, 2003, **62**, 227–236.
10. Sarma, J. N. and Phukan, M. K., Origin and some geomorphological changes of Majuli island of the Brahmaputra River in Assam, India, *Geomorphology*, 2004, **60**, 1–19.
11. Kotoky, P., Bezbaruah, D., Baruah, J. and Sarma, J. N., Nature of bank erosion along the Brahmaputra River channel, Assam, India. *Curr. Sci.*, 2005, **88**, 634–640.
12. Thorne, C. R., Russel, A. P. G. and Alam, M. K., Planform pattern and channel evolution of the Brahmaputra river, Bangladesh. In *Braided Rivers* (eds Best, J. L. and Bristow, C. S.), Geol. Soc., London, 1993, pp. 257–276.
13. Sarker, M. H., Huque, I., Alam, M. and Koudstaal, R., Rivers, chars, and char dwellers of Bangladesh. *Int. J. River Basin Manag.*, 2003, **1**, 61–80.
14. Baki, A. B. M. and Gan, T. W., Riverbank migration and island dynamics of the braided Jamuna River of the Ganges-Brahmaputra basin using multi-temporal Landsat images. *Q. Intl.*, 2012, **263**, 148–161.
15. Uddin, M. N. and Rahman, M., Flow and erosion at a bend in the braided Jamuna river. *Intl. J. Sediment Res.*, 2012, **27**, 498–509.
16. Lahiri, S. K. and Sinha, R., Morphotectonic evolution of the Majuli Island in the Brahmaputra valley of Assam, India inferred from geomorphic and geophysical analysis. *Geomorphology*, 2014, **227**, 101–111.
17. Lahiri, S. K. and Sinha, R., Application of fast fourier transform in fluvial dynamics in the upper Brahmaputra valley, Assam. *Curr. Sci.*, 2015, **108**, 90–95.
18. Takagi, T., Oguchi, T., Matsumoto, J., Grossman, M. J., Sarker, M. H. and Matin, M. A., Channel braiding and stability of the

Brahmaputra river, Bangladesh, since 1967: GIS and remote sensing analysis. *Geomorphology*, 2007, **85**, 294–305.
19. Chembolu, V. and Dutta, S., Entropy and energy dissipation of a braided river system. *Procedia Eng.*, 2016, **144**, 1175–1179.
20. Karmaker, T., Ramprasad, Y. and Dutta, S., Sediment transport in an active erodible channel bend of Brahmaputra river. *Sadhana*, 2010, **35**, 693–706.
21. Goswami, D. C., Brahmaputra river, Assam, India: physiography, basin denundation and channel aggradation. *Water Resour. Res.*, 1985, **21**, 959–978.
22. WAPCOS [Water and Power Consultancy Services (India)], Morphological Studies of the River Brahmaputra. North Eastern Council, Govt of India, New Delhi, 1993, pp. I-1–IX-131.
23. Karmaker, T. and Dutta, S., Erodibility of fine soils from the composite bank of Brahmaputra river in India. *Hydrol. Processes*, 2011, **25**, 104–111.
24. Karmaker, T. and Dutta, S., Modeling seepage erosion and bank retreat in a composite river bank. *J. Hydrol.*, 2014, **476**, 178–187.
25. Karmaker, T. and Dutta, S., Stochastic erosion of composite banks in alluvial river bends. *Hydrol. Processes*, 2015, **29**, 1324–1339.
26. EGIS (Environmental and GIS Support Project for Water Sector Planning), Morphological Dynamics of the Brahmaputra–Jamuna River. Prepared for Water Resources Planning Organization, Dhaka, Bangladesh, 1997.
27. Sarkar, A., Garg, R. D. and Sharma, N., RS-GIS based assessment of river dynamics of Brahmaputra river in India. *J. Water Resour. Prot.*, 2012, **4**, 63–72.
28. Torrence, C. and Compo, G., A practical guide to wavelet analysis. *Bull. Am. Meteorol. Soc.*, 1998, **79**, 61–78.
29. Mount, N. J., Tate, N. J., Sarker, M. H. and Thorne, C. R., Evolutionary, multi-scale analysis of river bank line retreat using continuous wavelet transforms: Jamuna river, Bangladesh. *Geomorphology*, 2013, **183**, 82–95.
30. Brice, J. C., Channel pattern and terraces of the Loup river in Nebraska. *US Geol. Surv. Prof. Pap.*, 1964, **422D**, 1–41.
31. Chang, H. H., *Advanced Hydrology*, McGraw Hill Publisher, 1977.

ACKNOWLEDGEMENT. The authors thank reviewers for critically reviewing this paper and suggesting improvements.

Received 31 March 2016; revised accepted 11 September 2016

doi: 10.18520/cs/v112/i07/1533-1543